ACS Biomaterials SCIENCE & ENGINEERING

Article

Cite This: ACS Biomater. Sci. Eng. 2020, 6, 889−897

pubs.acs.org/journal/abseba

Migration of Microparticle-Containing Amoeba through Constricted Environments

Michael Timmermann,[†] Nils Lukat,[†] Lindsay P. Schneider,[†] C. Wyatt Shields, IV,[‡,§] Gabriel P. López,[‡,∥] and Christine Selhuber-Unkel*[,†]

[†]Institute of Materials Science, Biocompatible Nanomaterials, University of Kiel, Kaiserstr. 2, 24143 Kiel, Germany

[‡]NSF Research Triangle Materials Research Science and Engineering Center, Durham, North Carolina 27708, United States

[§]Department of Mechanical Engineering and Materials Science, Duke University, Durham, North Carolina 27708, United States

[∥]Center for Biomedical Engineering, Department of Chemical and Biological Engineering, University of New Mexico, Albuquerque, New Mexico 87131, United States

Supporting Information

ABSTRACT: In many situations, cells migrate through tiny orifices. Examples include the extravasation of immune cells from the bloodstream for fighting infections, the infiltration of cancer cells during metastasis, and the migration of human pathogens. An extremely motile and medically relevant type of human pathogen is *Acanthamoeba castellanii*. In the study presented here, we investigated how a combination of microparticles and microstructured interfaces controls the migration of *A. castellanii* trophozoites. The microinterfaces comprised well-defined micropillar arrays, and the trophozoites easily migrated through the given constrictions by adapting the shape and size of their intracellular vacuoles and by adapting intracellular motion. After feeding the trophozoite cells in microinterfaces with synthetic, stiff microparticles of various sizes and shapes, their behavior changed drastically: if the particles were smaller than the micropillar gap, migration was still possible. If the cells incorporated particles larger than the pillar gap, they could become immobilized but could also display remarkable problem-solving capabilities. For example, they turned rod-shaped microparticles such that their short axis fit through the pillar gap or they transported the particles above the structure. As migration is a crucial contribution to *A. castellanii* pathogenicity and is also relevant to other biological processes in microenvironments, such as cancer metastasis, our results provide an interesting strategy for controlling the migration of cells containing intracellular particles by microstructured interfaces that serve as migration-limiting environments.

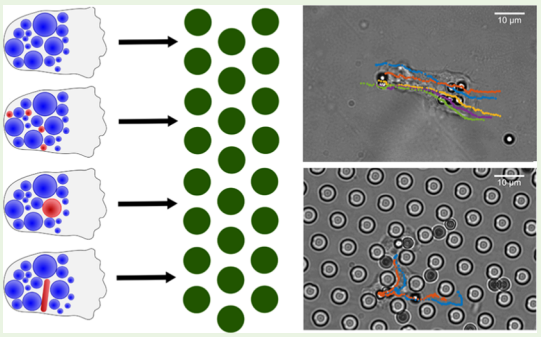

KEYWORDS: *microstructures, microspheres, microrods, biomaterial, human pathogens, cell motility*

INTRODUCTION

Cells live in diverse natural environments. In many such environments, it is crucial that cells have the ability to migrate and squeeze through tiny orifices. Examples include the extravasation of leukocytes from blood vessels to reach sites of inflammation,[1] the metastasis of cancer cells in the body,[2,3] the migration of protozoa residing in the soil,[4] and the migration of the social amoeba *Dictyostelium discoideum*.[5] Although many amoeba species are harmless, there are also human pathogenic species that rely on migrating to their host or inside the host tissue, thus making them interesting candidates for study in a biomedical context. For example, the causative agent of amoebiasis, *Entamoeba histolytica*, strongly relies on migration for the invading tissue.[6] Another species, *Acanthamoeba castellanii*, can evoke several severe diseases in the eye and the brain.[7] Trophozoites of this amoeba are highly motile and can migrate through microchannels in hydrogels,[8] although their intracellular space is supercrowded.[9] As migration is essential for the pathogenic activity of the acanthamoeba trophozoites, controlling this parameter could lead to infection-preventing strategies.

In addition, *Acanthamoeba*-borne diseases are believed to be caused, in part, by their phagocytic nature,[10] where actin rearrangement plays a major role.[11] Trophozoites of *A. castellanii* are highly phagocytic and easily take up extracellular targets, for example, red blood cells[12] and micron-sized latex beads[13] into their cytoplasm, where they are actively driven within the supercrowded cytoplasm.[9] In this work, we sought (i) to study the migration of *A. castellanii* trophozoites through constricted microenvironments and (ii) to temper their movements via the ingestion of microparticles with well-defined size and shape (Figure 1). By understanding and controlling their migration, novel material-based strategies for preventing *Acanthamoeba*-borne diseases which are based on

Received: April 10, 2019
Accepted: November 30, 2019
Published: November 30, 2019

DOI: 10.1021/acsbiomaterials.9b00496
ACS Biomater. Sci. Eng. 2020, 6, 889−897

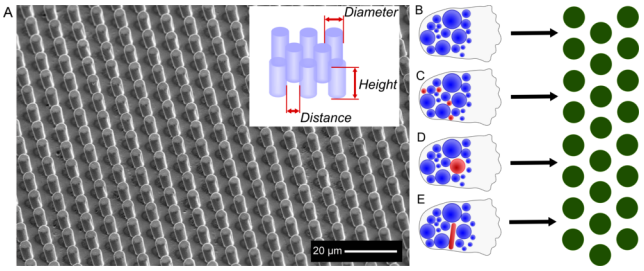

Figure 1. SEM image of the micropatterned environment with well-defined diameter, distance, and height of pillars through which the amoeba traversed (A) and sketch of the different cases of loading that were observed in the studies. Amoeba entering the microstructured interface without additional loading (B), with spheres smaller than the micropillar gap (C), with spheres larger than the gap (D), and with rods with a diameter smaller and a length larger than the gap (E).

capturing the parasite before entering the body may be developed.

We demonstrate several adaptive strategies of *A. castellanii* trophozoites when migrating through constricted microstructured interfaces. Further on, we employed synthetic microparticles to fill their intracellular space and thus modulate their movement by the combination with microstructured interfaces. In the experiments, particle size was chosen such that it was either below or above the gap size of the predefined microenvironments. Our results show that *A. castellanii* trophozoites can employ several problem-solving strategies to navigate narrow constrictions. The goal of this part of the study was to qualitatively document these events and describe the different strategies employed by the *A. castellanii* trophozoites.

RESULTS

***A. castellanii* Trophozoites Adapt Their Vacuoles to Constrictions.** To study the interaction of *A. castellanii* trophozoites, we fabricated microenvironments in the form of polydimethylsiloxane (PDMS) micropillars. The wall-to-wall distance of neighboring pillars was 5.5 μm, the pillar height was 10 μm, and the pillar diameter was 4.5 μm. With an interpillar distance of 5.5 μm, we chose a gap size that is in the size range of the larger vacuoles in the trophozoites and is in the size range of gap sizes provided by the extracellular matrix.[2] Hence, we first analyzed how the intracellular space of the trophozoites, which is densely packed with vacuoles, is influenced by spatial confinement. As a control, we chose a flat PDMS surface on which *A. castellanii* trophozoites readily spread and migrated.

Figure 2A shows a representative example of an *A. castellanii* trophozoite with large vacuoles migrating on a flat, unstructured PDMS sample. By comparing Figure 2A,B, it is discernible that the projected vacuole diameter is smaller inside of the PDMS micropattern than that inside of the unpatterned sample. To quantify this difference, we measured the projected diameter of the largest vacuole of cells both inside and outside of the pillar structure. As shown in Figure 2C, the projected diameter of the largest intracellular vacuole of *A. castellanii* inside of the microstructured interface was significantly smaller than that on flat PDMS. Geometrical considerations show that the maximum interior circle fitting between pillars has a diameter of 7 μm. Clearly, except for one outlier, all measured vacuole diameters are below 7 μm and the majority of measured diameters is even smaller than the size of the pillar gap of 5.5 μm. This result suggests that *A. castellanii* trophozoites adapt the size of their largest vacuole to the available space in the micropattern. We note that we did not observe any significant deviations in vacuole shape.

In addition to changes in vacuole size, also the shape of the trophozoites is different on flat compared to micropatterned PDMS surfaces. While the *A. castellanii* trophozoites mostly adopt a roundish to elliptical shape outside of the micropatterns, they acquire a more elongated shape with a serpentine-like outline inside of the micropillar arrays. This shape adaptation is clearly manifested by a change in their circularity (Figure 2D).

***A. castellanii* Trophozoite Migration through Micropillars is Controlled by the Size of Phagocytosed Particles.** While vacuoles appear to be adaptive organelles,[14] particles made of synthetic polymers such as polystyrene and SU-8 do not readily deform by forces on the cellular scale. To challenge the cells, we investigated how *A. castellanii* trophozoites navigate the spatial confinement of micropillar structures after phagocytosing different types of synthetic particles. It is important to note that the phagocytosis of particles did not cause apparent morphological changes to the trophozoites (Figure 3). On the one hand, we used spherical particles that had a diameter of 3 μm, thus being smaller than the 5.5 μm wall-to-wall distance between pillars. On the other hand, we used spherical particles with a diameter of 6.7 μm,

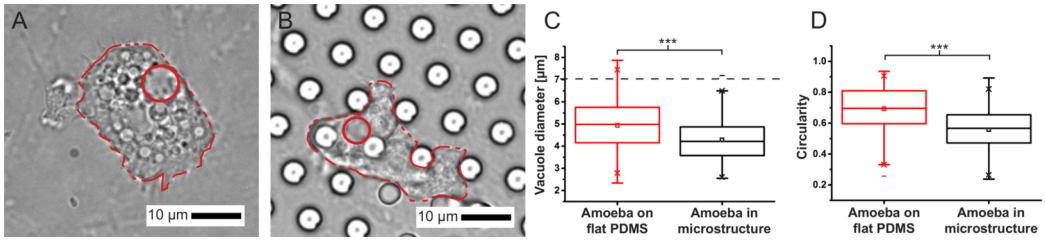

Figure 2. Phase contrast microscopy images of representative *A. castellanii* trophozoites on a flat (A) and on a micropatterned (B) PDMS substrate. Dashed red line marks the outline of the trophozoite, while the continuous red line marks the outline of the largest intracellular vacuole. Cells are rounder on the flat PDMS substrate than on the micropatterned surface, where the cell is spread between the pillars in different directions. Inside of the micropattern, the size of the vacuole is limited by the maximum size of the interior circle fitting between two adjacent pillars (dashed line in c). Box plot (C; box: interquartile range; line in each box: median; dot: mean; whiskers: minimum/maximum) shows a significant difference between the size of the largest vacuoles of cells inside and outside of the micropattern ($p < 0.001$, ***, Student's *t*-test, 109 cells analyzed on flat PDMS, 114 cells analyzed in the micropillar array). Same holds for the circularity of the amoeba (D; box: interquartile range; line in each box: median; dot: mean; whiskers: minimum/maximum). There is a significant difference between the circularity of the amoeba inside and outside of the micropattern ($p < 0.001$, ***, Student's *t*-test, 109 cells analyzed on flat PDMS, 114 cells analyzed in the micropillar array).

DOI: 10.1021/acsbiomaterials.9b00496
ACS Biomater. Sci. Eng. 2020, 6, 889−897

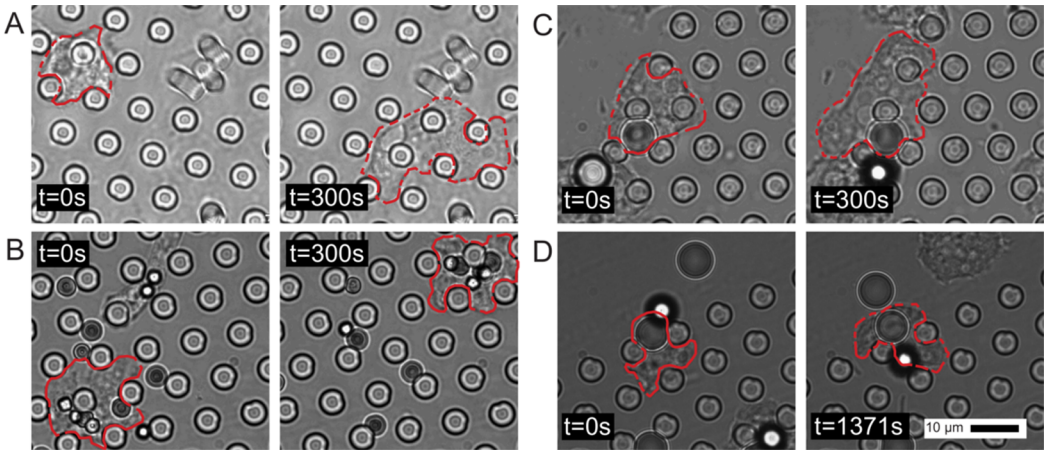

Figure 3. *A. castellanii* inside the micropattern without particles (A), with particles smaller than the pillar gap (B), and with particles larger than the pillar gap (C,D). In all four situations, the cell shape adapts to the micropattern given by the pillars. Snapshots at 0 and 300 s (C) and at 0 and ~1371 s (D) demonstrate that cell migration is strongly hindered in (C,D).

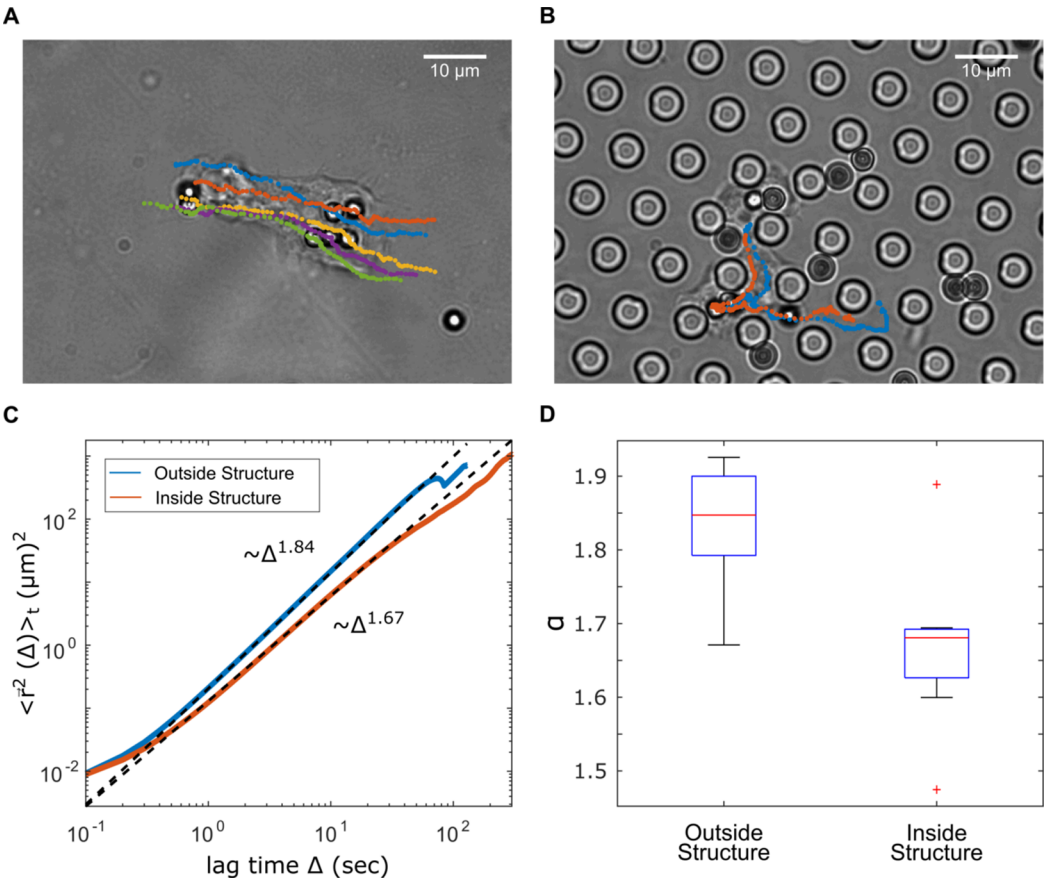

Figure 4. Motion of phagocytosed spherical beads (diameter: 3 μm). (A) Phase-contrast image of an *A. castellanii* tropohzoite containing several beads outside of the micropillar array and (B) inside of the array. Exemplary bead trajectories are highlighted. (C) MSD of beads, averaged over 10 single MSDs outside and 8 single MSDs inside of the structure. (D) Box plots of the distribution of the diffusion exponent of single MSDs recorded from intracellular beads inside and outside of the structure. (box: 25th and 75th percentiles; red line: median; whiskers: minimum/maximum; "+": outlier).

thus exceeding the wall-to-wall distance between pillars. Figure 3B and Supplementary Movie 2 show that *A. castellanii* trophozoites carrying intracellular particles smaller than the pillar gap can easily migrate between micropillars. In contrast, cells that had internalized particles larger than the interpillar gap were drastically hindered in their movement (Figure 3C and Supplementary Movie 3). For example, in Figure 3C, the cell rather moved its main body around, while the particle was stuck between the pillars. This resulted in cellular jamming or cells not entering the structure at all (Figure 3D and Supplementary Movie 6) in most situations. The longest timeframe we observed was 1371 s.

Intracellular Microparticle Motion is Hindered by the Microstructured Interfaces. It has recently been shown that

DOI: 10.1021/acsbiomaterials.9b00496
ACS Biomater. Sci. Eng. 2020, 6, 889−897

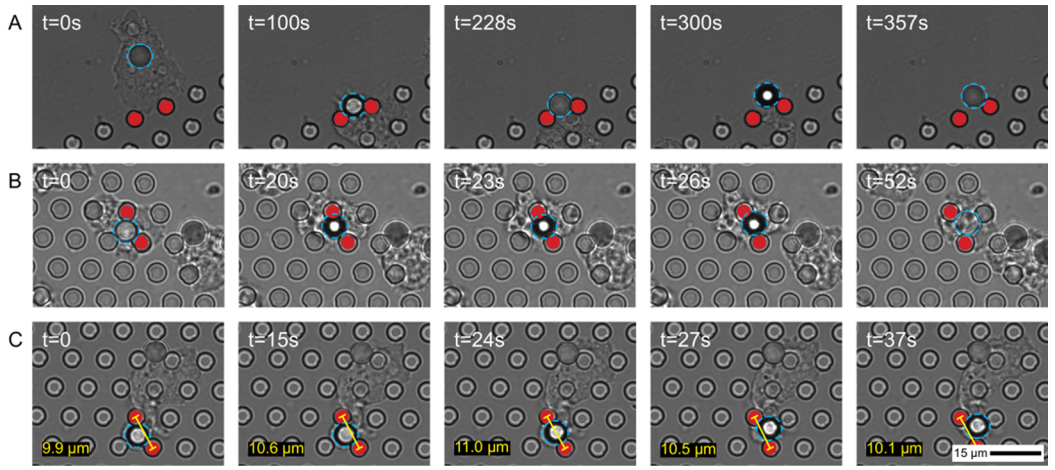

Figure 5. Strategies of *A. castellanii* to bypass micropillar structures after phagocytosing a particle larger than the gap between two adjacent pillars. Images in (A–C) show snapshots at different time points for three different cellular strategies. Each row shows different cellular strategies: the cell (A) ejects the particle, (B) carries the particle over the structure, and (C) pulls the particle through the opening by exerting forces. To aid in visualization, the pillar constrictions of interest are marked with red dots. Particles of interest are encircled with a blue dotted line. In (C), the size of the pillar gap is marked by yellow lines and its length is given.

intracellular motion within *A. castellanii* trophozoites is superdiffusive and strongly relies on the actin-myosin system.[9] Particles smaller than the pillar gap traversed easily through the microstructure, whereas larger phagocytosed microparticles could make the trophozoites stuck in the structure. To quantify the effect of the micropillar array on the motion of the amoeba, it would be useful to track the amoeba directly. Unfortunately, this is not possible because the determination of the boundary of the amoeba inside the micropillar structure is not accurate. For amoeba on flat surfaces, the motion of the phagocytosed particle is a good marker for the total motion of the amoeba (Figure 4A). Still, the motion of the particle is a superposition of two parts: the motion of the amoeba and intracellular motion. The influence of amoeba motion obviously dominates outside of the micropillar structure, as shown in Figure 4A, where the trajectories of five intracellular particles on flat PDMS are shown. Here, the particles are clearly driven in the direction of movement of the amoeba. In order to investigate the influence of the micropillar arrays on particle motion, we tracked their position via time-lapse imaging. The resulting trajectories are shown in Figure 4B. To study the effect of the micropillar environment on particle motion, we determined the mean-squared displacement (MSD) of the intracellular particle trajectories using the concept of anomalous diffusion: the MSD is $\langle r^2 \rangle \propto t^{\alpha}$, with t being the lag time (Figure 4C). α = 1 resembles Brownian motion, which is not applicable here because of the strong active motion present. Instead, active motion is represented by $\alpha > 1$, and subdiffusion would lead to $\alpha < 1$. Here, we analyzed five amoeba and 18 trajectories of intracellular particles (8 inside and 10 outside of the PDMS micropillar structure). The MSDs for these trajectories are shown in Figure 4C, demonstrating that phagocytosed microparticles (diameter: 3 μm) move superdiffusively with a diffusive exponent of $\alpha = 1.84 \pm 0.08$ ($N = 10$) if the trophozoite is migrating on a flat, unstructured PDMS substrate. This result demonstrates that active intracellular motion is dominating. Phagocytosed microparticles inside trophozoites, which are traveling through the micropillar structure, resulted in a smaller diffusive exponent of $\alpha = 1.67 \pm 0.11$ ($N = 8$). A more detailed view of the diffusive exponent is shown in Figure 4D. Here, a box plot is representing the diffusive exponent of single particles. The red central mark is the median, and the bottom and top edges of the box show the 25th and 75th percentiles, respectively. The whiskers extend to the most extreme data points not considered as outliers, and the outliers are displayed with the "+" symbol.

Cells Can Overcome Jamming in Microstructure Interfaces. After the phagocytosis of larger particles (diameter: 6.7 μm), the microstructure could impair cellular motion. Yet in some cases that we documented qualitatively, the cells were still able to invade the micropillar array and migrate within via multiple problem-solving strategies. In detail, we observed the following problem-solving strategies: (1) the internalized particle was exocytosed, and the trophozoite continued its migration without the particle, (2) the internalized particle was transported above the pillar structure, and (3) the pillars were deformed such that the internalized particle could be pulled through the widened gap (Figure 5).

In the first case, which we documented once (Figure 5A, Supplementary Movie 5), the trophozoite tried to invade the array. As the microbead did not fit between the pillars, it remained in the back of the cell and thus outside of the array. The large particle hindered the cell from entering the array, and the trophozoite exocytosed the particle and then invaded the array without the particle. The particle remained outside of the micropattern. In the second case, which we documented four times (Figure 5B, Supplementary Movie 4), the cell exploited the fact that the array is not closed on the top. The cell carried the particle above the pillars (i.e., 10 μm), as is evident by its movement outside of the focal plane and thus avoided confinement. In the third case, which we documented twice (Figure 5C, Supplementary Movie 7), the cell dragged the particle between two pillars and applied considerable force. As a result of the flexibility of the PDMS, the pillars could bend and the particle was pulled through. The pictures in Figure 5C show that each of the two pillars deformed by about 0.55 μm. From the 2D pictures, it is not possible to see the precise point of contact between the cells and pillars, thus the exact force applied cannot be determined. However, this point can neither be lower than the radius of the bead (3.35 μm) nor higher than the pillar itself (10 μm). This leads to a force between 75 nN

DOI: 10.1021/acsbiomaterials.9b00496
ACS Biomater. Sci. Eng. 2020, 6, 889–897

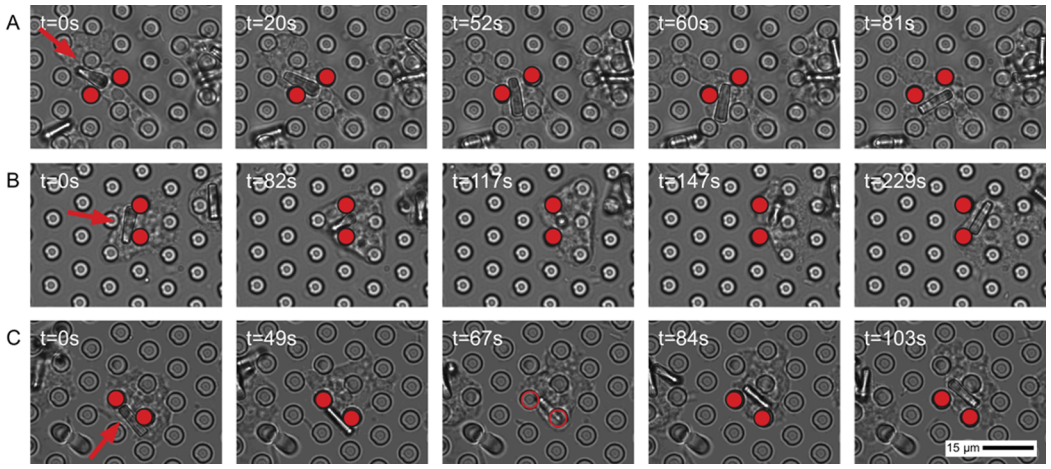

Figure 6. *A. castellanii* migrating through the micropillar array after phagocytosing a cylindrical particle with a diameter smaller than the gap between pillars, but a length larger than the gap. Three different scenarios were observed. Cell (A) guides the rod through the structure by turning it parallel to the surface (oriented in the direction of motion), (B) turns the rod perpendicular to the surface before guiding it through the pillars, or (C) carries the rod above the structure. Opening between pillars is marked with red dots. Location of the particle is indicated by a red arrow in the first frame of each phase contrast image sequence.

(at 10 μm) and 920 nN (at 3.35 μm). As the contact of the cell with the pillars is presumably a continuum contact, we estimate that the pushing force is in the range of several 100 nN. Still, we have observed a preference for carrying the particles over the micropattern.

Rod-Shaped Particles Are Transported According to the Structural Features of the Pillar Micropattern. To study the navigation of cells with internalized asymmetric particles through constrictions, we fabricated quasi-cylindrical microrods with a diameter smaller, but a length larger, than the micropillar gap (length: 10 μm, diameter: 2 μm).

Three different strategies for transporting cylindrical microparticles through the pillar array were observed (Figure 6). In the first case, the particle was guided through the opening between two pillars with its short diameter leading through the gap between the pillars. Its long axis remained parallel to the surface throughout the process (Figure 6A). In the second case, the rod turned from being parallel to the surface to perpendicular before entering an opening between two pillars. The particle was then guided through the opening easily, as its diameter is much smaller than the gap. After the gap, the particle was again turned parallel to the surface (Figure 6B). In the third case, the rod remained parallel to the surface but was carried above the pillars (Figure 6C), similar to the situation for spherical particles shown in Figure 5B. In total, we documented 16 amoeba containing rod-shaped particles. One carried the particle above the structure, 4 twisted the particle to get it through the obstacle, 11 guided it through the gap, and one did not move at all. Hence, we observed a preference for guiding the particles through the pillar structure instead of transporting them above. This transport appears to be very directed and well-organized (Supplementary Movies 9 and 10).

DISCUSSION

We have used time-lapse imaging to study the effect of intracellular cargo on the migration of the human pathogen *A. castellanii* in constricted environments. Whereas it is well known that micro and nanotopographies can control the migration of cells[15−17] and pathogens,[18,19] we here focus on the combined impact of microtopographies and the shape and size of intracellular cargo in the form of phagocytosed synthetic microparticles.

Recently, it has been shown that the nucleus of cells is a decisive factor in determining if cells are able to move through confining environments.[20] Although the nucleus is a relatively stiff cellular object, it is still dynamic and adaptive in that it can open and reseal during cell migration through narrow gaps.[2] In *A. castellanii* trophozoites, one might assume that their motion through tiny constrictions is hindered by the largest vacuole in their supercrowded cytoplasm. However, we observed that the vacuoles were adapted to the size of the pillar gap, thus showing the ability of these human pathogens to adapt to various structures in their environment. In addition to the geometric blockage of cell migration by a large cellular object such as the nucleus, other aspects such as adhesiveness, contractility, and cell stiffness have been discussed.[21] In our experiments, the adhesion between PDMS and cells can be expected to be the same all over the array. However, we cannot exclude the possibility that cell adhesion, stiffness, and contractility are different inside and outside of the array. This could contribute to the adaption of vacuole size inside the micropillar structures.

Qualitatively, our observations showed that the micropillars rather provided obstacles for cell migration. This was also manifested by the impact of micropillars on the motion of intracellular particles. The particles move inside the amoeba and are actively driven, but the cavities between micropillars appear to catch them and the transition between such cavities is fast and straight. The situation is reminiscent of particles moving in porous actin networks.[22] Characterizing the intracellular motion in *A. castellanii* is important as it contributes to its pathogenicity, and active transport is a dominant contribution.[23,24] However, it is important to note here that the values of the diffusive exponent mentioned in the Results section are absolute values of intracellular motion and thus also include absolute cell motion; however, it is possible to separate these aspects outside of micropillar structures,[9] this is not possible here because of the nonuniform shape of the cellular outline. Hence, our result that particle motion is changed inside the micropattern also reflects that cell motion is hindered inside the micropattern. Still, our result is similar to

DOI: 10.1021/acsbiomaterials.9b00496
ACS Biomater. Sci. Eng. 2020, 6, 889−897

the diffusive exponent determined for endogenous intracellular vacuoles,[9] where it had been shown that cellular motion strongly drives intracellular motion in *A. castellanii* trophozoites.

A particularly remarkable result of our investigations is how the trophozoites adapt to situations where they had phagocytosed synthetic particles larger than the size of the pillar gap. Either the cells got immobilized or they found unexpected ways to continue migrating in spite of being hindered by the micropillar array. Three strategies were most noteworthy. First, the pillars were bent by cellular forces in the range of several 100 nN. This force is realistic, as forces in a similar range have been measured for cardiomyocytes in micropillar structures.[25] Second, cargo was transported above the micropillar array to avoid hindrance by obstacles. Of course, the latter transport mode is only possible if the structures are not sealed on top, but it shows that the trophozoites can detect the free space and reposition their cargo accordingly. Third, rod-shaped particles were turned around to fit through the gaps. Here, the geometric anisotropy of the rod-shaped particles allowed us to observe rotational effects, which is normally only possible using, e.g., Janus particles.[26] The interpretation of these observations, which we regard as "problem-solving" is complex. Recently, it was reported that the social amoeba *D. discoideum*, which is a common biophysical model system for amoeba, switches between random motion and directed motion.[15] As the pillars provide a structurally asymmetric environment to cells, we assume that they test the structure by random motion and sometimes manage to overcome the obstacles (e.g., by transporting the particle above the structure). An indeed interesting case is the rotation of the rod-shaped particles so that they fit through the gaps. Here, the symmetry of the hexagonally arranged pillars might simplify the case: If the rod once fit through the pillars, it just needs to be transported in a directional way. Directed motion of amoeba in pillar landscapes (without phagocytosed particles) has recently been reported.[27] Indeed, this type of "problem-solving" may therefore be a consequence of random motion, and future work must be carried out to explore if this is an intentional or random process. As cells are also able to exert forces to their surroundings,[28] it is not a surprise that cells sometimes even took the direct way to press the particle through the pillars.

Interestingly, it has recently been discussed that global and local cell geometry could be sensed by the cytoskeleton, reaction-diffusion systems or molecular complexes.[29] Similar concepts have already been discussed and proven for geometry sensing in cell adhesion,[30] again supporting the notion of a cell acting as an intelligent system. The idea that cells are able to solve complex problems has already been discussed in the context of biochemical processes and cell memory[31] and could in the future also be a highly interesting context to be exploited in bioengineering and biomaterials design.

CONCLUSIONS

Our data demonstrate that the size and shape of phagocytosed microparticles can be employed to control *A. castellanii* migration in constricted microenvironments. This result may provide a novel strategy for preventing *Acanthmoeba*-borne diseases by capturing them in artificial microenvironments through the combination with synthetic particles to generate novel filtering or cleaning devices. In addition, the results also have a broader impact on other cell systems that rely on migration. A particularly interesting aspect is tumor metastasis, where cells migrate through the dense extracellular matrix to reach sites for secondary tumor formation. The strategy of employing microparticles to immobilize cells could therefore also provide novel routes for therapy in this field.

MATERIALS AND METHODS

Template Preparation. The silicon master template was fabricated from a 4 inch silicon wafer (1 0 0). After a 5 min prebake at 200 °C on a hotplate and a cool down time of 10 min, the wafer was spin-coated with 4 mL of negative photoresist (SU-8 10, MicroChem Corp., USA) via a two-step process: a five s step at 500 rpm with a speed ramp of 100 rpm/s, followed by a 27 s step at 2000 rpm with a speed ramp of 3000 rpm/s. The wafer was then placed on a hotplate at 65 °C for 2 min for the soft-bake. This plate, with the wafer still on top, was adjusted to 95 °C, and once it reached the temperature, the soft-bake process was finished by baking for 5 more minutes. After cooling for 5 min, the resist was exposed to UV light at 1500 mJ/cm^2 in a mask-aligner (MA6/BA6, Süss Microtec, Germany) through a chromium-printed mask. The mask contained full circles in a hexagonal pattern, with a spacing of circle centers of 10 μm and a diameter of 4.5 μm. A postexposure bake was conducted similar to the soft-bake, with only 1 min at 65 °C and 2 min at 95 °C. The cooled wafer was then developed for 2 min in an SU-8 developer (MicroChem Corp., USA), rinsed with propan-2-ol (Sigma-Aldrich GmbH, Germany), blow-dried with nitrogen, and hard-baked at 200 °C for 5 min. In the end, the wafer was cut into approximately 1 × 1 cm^2 pieces including 3 × 3 mm^2 areas of the desired features.

Polymer Molding. PDMS is a silicone often used for generating microstructures through molding.[32] To prevent the sticking of cured PDMS to the silicon-based master templates, the templates were silanized with trichloro(1*H*,1*H*,2*H*,2*H*-perfluorooctyl)silane (Sigma-Aldrich GmbH, Germany) by placing two droplets of silane solution onto a 1 cm^2 wafer piece and placing them in a desiccator under vacuum for 2 h. PDMS prepolymer solution and curing agent were prepared in a 10:1 (w/w) ratio (Sylgard 184, Dow Corning, USA), degassed for 1 h in a desiccator, and poured on a glass slide. A silicon template with the microstructure features facing downward was placed on the polymer, and a gentle pressure was applied to decrease the thickness of PDMS between the template and the glass slide. This assembly was degassed in a desiccator for 10 min, in order to release the air from the template, force the PDMS inside the features, and remove the last few air bubbles in the PDMS. Subsequently, the PDMS was cured in an oven for 1 h at 65 °C. While still warm, the template was detached from the PDMS with plastic tweezers. This preparation resulted in PDMS pillars of approximately 10 μm height.

Preparation of SU-8 Rods. The methods of fabricating the microrods have been described elsewhere.[33,34] Briefly, we spin coated SU-8 10 (MicroChem Corp.) on 3 in. single-side polished silicon wafers (Addison Engineering, Inc.), exposed the resist to a chrome-printed photomask containing 2 μm transparent pores (365 nm, MA/BA6 Mask Aligner, Süss MicroTec AG), and developed the photoresist using procedures provided by MicroChem.[34,35] The wafers were rinsed with steady streams of acetone and methanol and were then carefully dried with nitrogen gas. Particles were then removed from the wafers via shear forces from a rubber policeman. Finally, particles were suspended in 0.5 vol % Tween 20 in deionized water at a concentration of ~2.2 × 10^8 particles/mL.

Microparticle Solution Preparation. In our experiments, different types of microparticles were used for phagocytosis: polystyrene spheres with diameters of 6.7 μm (PC-S-6.0, Kisker Biotech GmbH &Co. KG, Germany) and 3 μm (Polysciences, Inc.) and cylindrical SU-8 microrods with a length of 10 μm and a diameter of 2 μm. To create suspensions of microparticles, 200 μL of stock polystyrene particle solution was mixed with deionized water in a 1:4 (v/v) ratio. For SU-8 particles, 25 μL of the original solution (containing ~2.2 × 10^8 particles suspended in 1 mL of 0.5 vol % Tween 20 in deionized water) was mixed with deionized water in a 1:9 (v/v) ratio. All three solutions were washed three times by

DOI: 10.1021/acsbiomaterials.9b00496
ACS Biomater. Sci. Eng. 2020, 6, 889−897

centrifuging for 15 min with 6236*g* in a centrifuge (Mikro 220r, Andreas Hettich GmbH & Co.KG, Germany) and replacing the liquid with 1 mL deionized water. After the third washing step, the water was replaced by 200 μL Peptone Yeast Glucose (PYG) 712 medium.

***Acanthamoeba* Experiments.** Trophozoites of *A. castellanii* (ATTC 30234) were cultured in PYG 712 medium at room temperature in 75 mL tissue culture bottles (Sarstedt, Germany), as described earlier.[36,37] For each experiment, a PDMS pillar array was detached from the glass slide and placed onto the bottom of a glass Petri dish (ibidi GmbH, Germany). A 100 μL solution containing spherical particles, 200 μL of solution containing rod-shaped particles or no solution was added to the dish, depending on the experiment. *A. castellanii* were detached from the cell culture substrate by striking the container and shaking it vigorously. The acanthamoebae were counted with a Neubauer hemocytometer, and 20 000 cells were incubated in the Petri dish in 1 mL PYG 712 medium for 15 h to ensure that the amoeba phagocytosed enough particles and that the medium sufficiently wet the hydrophobic PDMS micropattern. In total, 33 movies of *A. castellanii* migrating on the samples were collected using a 60× oil immersion objective (UPlanSApo 60× Oil, Olympus, Japan) on an inverted microscope (IX-81, Olympus, Japan) and a digital camera (Hamamatsu C9300, Hamamatsu, Japan) at 10 fps.

Calculation of Bending Forces. The force that the amoeba applies for bending pillars was calculated using the elementary beam theory to determine the force used to deform a beam with a round cross-section k_{bend} (eq 1). In order to calculate the correct bending force F from the measured deformation of the pillar, we took into account a correction factor *corr* proposed by Schoen et al. that includes the deformation of the substrate (eq 2–4).[28] By multiplying the calculated force F by two, the amount of force F_{cell} the cell is able to apply on one microparticle is calculated (eq 2). For the pillars used in this work, the following constants used were pillar diameter D = 4.5 μm and the length L = 10 μm (determined by micropillar preparation), the displacement of the pillar δ (determined by image analysis), the Young's modulus E = 1.72 MPa (from ref 38), a fitting parameter a = 1.3 (from ref 28), and the Poisson's ratio ν = 0.5 (from ref 39).

$$k_{bend} = \frac{3\pi E D^4}{64 L^3} \tag{1}$$

$$F_{cell} = 2F \tag{2}$$

$$F = \mathrm{corr} \times k_{bend}\delta \tag{3}$$

$$\mathrm{corr} = \frac{\frac{16}{3}\left(\frac{L}{D}\right)^3}{\left(\frac{16}{3}\left(\frac{L}{D}\right)^3 + \frac{7+6\nu}{3}\frac{L}{D} + 8a\frac{(1+\nu)}{2\pi}\left(2(1-\nu) + \left(1 - \frac{1}{4(1-\nu)}\right)\right)\left(\frac{L}{D}\right)^2\right)} \tag{4}$$

Image Analysis. Vacuole diameters, circularity of the cells, and the distance between pillars were determined with ImageJ (National Institutes of Health, USA).

The positions of phagocytosed particles were determined semi-automatically using a home-written Matlab (Mathworks, Inc.) segmentation algorithm, which is using two different strategies to detect particles. The first method is used if a particle is in focus, and it is based on detecting similar regions in consecutive frames of a video. The second method is used for out-of-focus particles and is based on the detection of white regions representing the particles. These white regions appear when the particle is located at a specific height with respect to the focus layer. The program selects the method of choice automatically. For verification, an xml file was created that can be read by the ImageJ plugin Mamut to verify that the particles were tracked correctly. In order to compare particle motion inside and outside of the micropillar structure, the absolute position of the particles was determined for both cases and used for the analysis. MSD analyses were carried out in Matlab using the tool msdanalyzer.[40] We determined the slope of the curves in log–log plots by taking into account the smallest 25% of all lag times in a specific MSD. Furthermore, only trajectories were taken into account that exhibited an exponential increase (linear in the log–log plot) in this interval. Four of the 22 trajectories did not fulfill this requirement and were therefore discarded.

Statistical Analysis. Statistical testing of vacuole size was conducted via a two-sample *t*-test in Origin 9.0 (OriginLab, Northampton, MA, USA).

■ ASSOCIATED CONTENT

Supporting Information

The Supporting Information is available free of charge at https://pubs.acs.org/doi/10.1021/acsbiomaterials.9b00496.

Sm_1: Amoeba moving through the pillar structure without any artificial particles inside (MP4)

Sm_2: Amoeba moving through the pillar structure with bead inside, bead diameter < pillar distance (MP4)

Sm_3: Amoeba trapped inside the structure with bead inside, bead diameter > pillar distance (MP4)

Sm_4: Amoeba carrying a bead over the pillar structure (MP4)

Sm_5: Amoeba exocytosing a bead to be able to enter the pillar structure (MP4)

Sm_6: Example of an amoeba not entering the pillar structure because bead it is too large (MP4)

Sm_7: Example of an amoeba bending pillars with the bead to get it across (MP4)

Sm_8: Example of an amoeba carrying a rod over the pillar structure (MP4)

Sm_9: Amoeba guiding a rod through the pillar gaps (MP4)

Sm_10: Example of an amoeba twisting the rod upward to guide it between pillars (MP4)

■ AUTHOR INFORMATION

Corresponding Author

*E-mail: cse@tf.uni-kiel.de.

ORCID

Gabriel P. López: 0000-0002-5383-0708

Christine Selhuber-Unkel: 0000-0002-5051-4822

Notes

The authors declare no competing financial interest.

■ ACKNOWLEDGMENTS

We acknowledge the funding from the European Research Council (starting grant 336104) and the German Research Foundation (SFB 1261, Project B7). We also acknowledge the funding support from the U.S. National Science Foundation's (NSF's) Research Triangle Materials Research Science and Engineering Center (MRSEC; DMR-1121107). Microrods were fabricated in the Shared Materials Instrumentation Facility (SMIF) at Duke University, which is a member of the North Carolina Research Triangle Nanotechnology Network (RTNN) and was supported by the NSF (grant no. ECCS-1542015) as part of the National Nanotechnology Coordinated Infrastructure (NNCI). L.S. was supported by the Deutscher Akademischer Austauschdienst (DAAD) through a RISE fellowship (Kiel_EN_1579). We thank Sören Gutekunst for fruitful discussions and Manuela Lieb for support in the lab.

DOI: 10.1021/acsbiomaterials.9b00496
ACS Biomater. Sci. Eng. 2020, 6, 889–897

■ ABBREVIATIONS

MSD, mean square displacement; PDMS, polydimethylsiloxane

■ REFERENCES

(1) Nourshargh, S.; Alon, R. Leukocyte Migration into Inflamed Tissues. *Immunity* **2014**, *41*, 694−707.

(2) Denais, C. M.; Gilbert, R. M.; Isermann, P.; McGregor, A. L.; te Lindert, M.; Weigelin, B.; Davidson, P. M.; Friedl, P.; Wolf, K.; Lammerding, J. Nuclear envelope rupture and repair during cancer cell migration. *Science* **2016**, *352*, 353.

(3) Friedl, P.; Gilmour, D. Collective cell migration in morphogenesis, regeneration and cancer. *Nat. Rev. Mol. Cell Biol.* **2009**, *10*, 445−457.

(4) Wang, W.; Shor, L. M.; LeBoeuf, E. J.; Wikswo, J. P.; Kosson, D. S. Mobility of Protozoa through Narrow Channels. *Appl. Environ. Microbiol.* **2005**, *71*, 4628−4637.

(5) Wang, C. J.; Bergmann, A.; Lin, B.; Kim, K.; Levchenko, A. Diverse Sensitivity Thresholds in Dynamic Signaling Responses by Social Amoebae. *Sci. Signaling* **2012**, *5*, ra17.

(6) Aguilar-Rojas, A.; Olivo-Marin, J.-C.; Guillen, N. The motility of Entamoeba histolytica: finding ways to understand intestinal amoebiasis. *Curr. Opin. Microbiol.* **2016**, *34*, 24−30.

(7) Marciano-Cabral, F.; Cabral, G. Acanthamoeba spp. as Agents of Disease in Humans. *Clin. Microbiol. Rev.* **2003**, *16*, 273−307.

(8) Gutekunst, S. B.; Siemsen, K.; Huth, S.; Möhring, A.; Hesseler, B.; Timmermann, M.; Paulowicz, I.; Mishra, Y. K.; Siebert, L.; Adelung, R.; Selhuber-Unkel, C. 3D Hydrogels Containing Interconnected Microchannels of Subcellular Size for Capturing Human Pathogenic Acanthamoeba Castellanii. *ACS Biomater. Sci. Eng.* **2019**, *5*, 1784.

(9) Reverey, J. F.; Jeon, J.-H.; Bao, H.; Leippe, M.; Metzler, R.; Selhuber-Unkel, C. Superdiffusion dominates intracellular particle motion in the supercrowded cytoplasm of pathogenic Acanthamoeba castellanii. *Sci. Rep.* **2015**, *5*, 11690.

(10) Vemuganti, G.; Sharma, S.; Athmanathan, S.; Garg, P. Keratocyte loss in Acanihamoeba Keratitis: Phagocytosis, necrosis or apoptosis? *Indian J. Ophthalmol.* **2000**, *48*, 291−294.

(11) Lorenzo-Morales, J.; Khan, N. A.; Walochnik, J. An update on Acanthamoeba keratitis: diagnosis, pathogenesis and treatment. *Parasite* **2015**, *22*, 10.

(12) Brown, R. C.; Bass, H.; Coombs, J. P. Carbohydrate binding proteins involved in phagocytosis by Acanthamoeba. *Nature* **1975**, *254*, 434.

(13) Avery, S. V.; Harwood, J. L.; Lloyd, D. Quantification and Characterization of Phagocytosis in the Soil Amoeba Acanthamoeba castellanii by Flow Cytometry. *Appl. Environ. Microbiol.* **1995**, *61*, 1124−1132.

(14) Desfougères, Y.; Neumann, H.; Mayer, A. Organelle size control − increasing vacuole content activates SNAREs to augment organelle volume through homotypic fusion. *J. Cell Sci.* **2016**, *129*, 2817−2828.

(15) Arcizet, D.; Capito, S.; Gorelashvili, M.; Leonhardt, C.; Vollmer, M.; Youssef, S.; Rappl, S.; Heinrich, D. Contact-controlled amoeboid motility induces dynamic cell trapping in 3D-microstructured surfaces. *Soft Matter* **2012**, *8*, 1473−1481.

(16) Nikkhah, M.; Edalat, F.; Manoucheri, S.; Khademhosseini, A. Engineering microscale topographies to control the cell−substrate interface. *Biomaterials* **2012**, *33*, 5230−5246.

(17) Driscoll, M. K.; Sun, X.; Guven, C.; Fourkas, J. T.; Losert, W. Cellular Contact Guidance through Dynamic Sensing of Nanotopography. *ACS Nano* **2014**, *8*, 3546−3555.

(18) Hellmann, J. K.; Münter, S.; Kudryashev, M.; Schulz, S.; Heiss, K.; Müller, A.-K.; Matuschewski, K.; Spatz, J. P.; Schwarz, U. S.; Frischknecht, F. Environmental Constraints Guide Migration of Malaria Parasites during Transmission. *PLoS Pathog.* **2011**, *7*, No. e1002080.

(19) Muthinja, J. M.; Ripp, J.; Krüger, T.; Imle, A.; Haraszti, T.; Fackler, O. T.; Spatz, J. P.; Engstler, M.; Frischknecht, F. Tailored environments to study motile cells and pathogens. *Cell. Microbiol.* **2018**, *20*, No. e12820.

(20) Davidson, P. M.; Denais, C.; Bakshi, M. C.; Lammerding, J. Nuclear Deformability Constitutes a Rate-Limiting Step During Cell Migration in 3-D Environments. *Cell. Mol. Bioeng.* **2014**, *7*, 293−306.

(21) Lautscham, L. A.; Kämmerer, C.; Lange, J. R.; Kolb, T.; Mark, C.; Schilling, A.; Strissel, P. L.; Strick, R.; Gluth, C.; Rowat, A. C.; Metzner, C.; Fabry, B. Migration in Confined 3D Environments Is Determined by a Combination of Adhesiveness, Nuclear Volume, Contractility, and Cell Stiffness. *Biophys. J.* **2015**, *109*, 900−913.

(22) Wong, I. Y.; Gardel, M. L.; Reichman, D. R.; Weeks, E. R.; Valentine, M. T.; Bausch, A. R.; Weitz, D. A. Anomalous Diffusion Probes Microstructure Dynamics of Entangled F-Actin Networks. *Phys. Rev. Lett.* **2004**, *92*, 178101.

(23) Brangwynne, C. P.; Koenderink, G. H.; MacKintosh, F. C.; Weitz, D. A. Intracellular transport by active diffusion. *Trends Cell Biol.* **2009**, *19*, 423−427.

(24) Thapa, S.; Lukat, N.; Selhuber-Unkel, C.; Cherstvy, A. G.; Metzler, R. Transient superdiffusion of polydisperse vacuoles in highly motile amoeboid cells. *J. Chem. Phys.* **2019**, *150*, 144901.

(25) Oyunbaatar, N.-E.; Lee, D.-H.; Patil, S.; Kim, E.-S.; Lee, D.-W. Biomechanical Characterization of Cardiomyocyte Using PDMS Pillar with Microgrooves. *Sensors* **2016**, *16*, 1258.

(26) Gao, Y.; Yu, Y.; Sanchez, L.; Yu, Y. Seeing the unseen: Imaging rotation in cells with designer anisotropic particles. *Micron* **2017**, *101*, 123−131.

(27) Gorelashvili, M.; Emmert, M.; Hodeck, K. F.; Heinrich, D. Amoeboid migration mode adaption in quasi-3D spatial density gradients of varying lattice geometry. *New J. Phys.* **2014**, *16*, 075012.

(28) Schoen, I.; Hu, W.; Klotzsch, E.; Vogel, V. Probing Cellular Traction Forces by Micropillar Arrays: Contribution of Substrate Warping to Pillar Deflection. *Nano Lett.* **2010**, *10*, 1823−1830.

(29) Haupt, A.; Minc, N. How cells sense their own shape − mechanisms to probe cell geometry and their implications in cellular organization and function. *J. Cell Sci.* **2018**, *131*, jcs214015.

(30) Vogel, V.; Sheetz, M. Local force and geometry sensing regulate cell functions. *Nat. Rev. Mol. Cell Biol.* **2006**, *7*, 265−275.

(31) Aquino, G.; Tweedy, L.; Heinrich, D.; Endres, R. G. Memory improves precision of cell sensing in fluctuating environments. *Sci. Rep.* **2014**, *4*, 5688.

(32) Tan, J. L.; Tien, J.; Pirone, D. M.; Gray, D. S.; Bhadriraju, K.; Chen, C. S. Cells lying on a bed of microneedles: An approach to isolate mechanical force. *Proc. Natl. Acad. Sci. U.S.A.* **2003**, *100*, 1484−1489.

(33) Wang, P.-Y.; Shields, C. W; Zhao, T.; Jami, H.; López, G.; Kingshott, P. Rapid Self-Assembly of Shaped Microtiles into Large, Close-Packed Crystalline Monolayers on Solid Surfaces. *Small* **2016**, *12*, 1309−1314.

(34) Shields, C. W., IV; Zhu, S.; Yang, Y.; Bharti, B.; Liu, J.; Yellen, B. B.; Velev, O. D.; Lopez, G. P. Field-directed assembly of patchy anisotropic microparticles with defined shape. *Soft Matter* **2013**, *9*, 9219−9229.

(35) Wang, P.-Y.; Shields, C. W.; Zhao, T.; Jami, H.; López, G. P.; Kingshott, P. Rapid Self-Assembly of Shaped Microtiles into Large, Close-Packed Crystalline Monolayers on Solid Surfaces. *Small* **2016**, *12*, 1309−1314.

(36) Reverey, J. F.; Fromme, R.; Leippe, M.; Selhuber-Unkel, C. In vitro adhesion of Acanthamoeba castellanii to soft contact lenses depends on water content and disinfection procedure. *Cont. Lens Anterior Eye* **2014**, *37*, 262−266.

(37) Gutekunst, S. B.; Grabosch, C.; Kovalev, A.; Gorb, S. N.; Selhuber-Unkel, C. Influence of the PDMS substrate stiffness on the adhesion of Acanthamoeba castellanii. *Beilstein J. Nantechnol.* **2014**, *5*, 1393−1398.

(38) Palchesko, R. N.; Zhang, L.; Sun, Y.; Feinberg, A. W. Development of Polydimethylsiloxane Substrates with Tunable Elastic

DOI: 10.1021/acsbiomaterials.9b00496
ACS Biomater. Sci. Eng. 2020, 6, 889−897

Modulus to Study Cell Mechanobiology in Muscle and Nerve. *PLoS One* **2012**, *7*, No. e51499.
(39) Pritchard, R. H.; Lava, P.; Debruyne, D.; Terentjev, E. M. Precise determination of the Poisson ratio in soft materials with 2D digital image correlation. *Soft Matter* **2013**, *9*, 6037−6045.
(40) Tarantino, N.; Tinevez, J.-Y.; Crowell, E. F.; Boisson, B.; Henriques, R.; Mhlanga, M.; Agou, F.; Israël, A.; Laplantine, E. TNF and IL-1 exhibit distinct ubiquitin requirements for inducing NEMO-IKK supramolecular structures. *J. Cell Biol.* **2014**, *204*, 231−245.

DOI: 10.1021/acsbiomaterials.9b00496
ACS Biomater. Sci. Eng. 2020, 6, 889−897